Dispersive Readout of Multilevel Systems

September 3, 2021

Contents

Reflectometry is a technique which enables spin readout of an electron without collapsing its wave-function, and can be used in a variety of systems. One such system in which reflectometry can be used measurement of the spin of a quantum dot [3]. Previous analysis of this system has been completed for a two level system coupled with a superconducting resonator [1], whereby the rotating wave approximation is used. In this report, a new formalism is introduced to investigate the transmission coefficient of a double quantum dot, which we treat as a three level system. Different systems are investigated and parameter sweeps are carried out to investigate the relationship between such parameters and the measurements observed.

1 System - Cavity Model

In this report, a system containing a double quantum dot, coupled to a superconducting resonator is investigated. A conceptual figure of this can be seen in Figure 1.

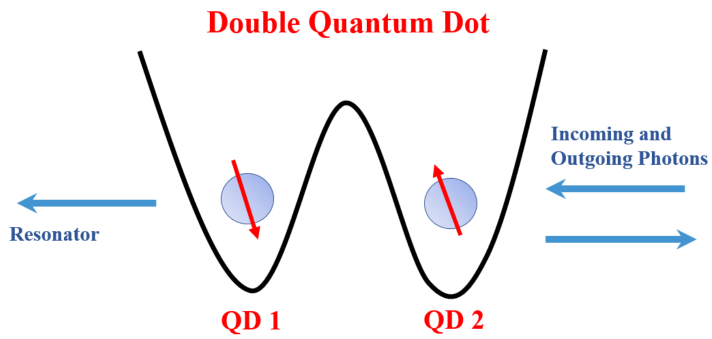

Figure 1: *Double Quantum Dot coupled to a superconducting resonator*

Initially, the two quantum dots can be in one of three states, corresponding to the two singlets or three degenerate triplet states. However, when we apply an external magnetic field to the system, the three degenerate triplet state splits into different states, as given below.

$$|S(0,2)\rangle = \frac{1}{\sqrt{2}}(|\Uparrow\Downarrow\rangle - |\Downarrow\Uparrow\rangle) \tag{1}$$
$$|S(1,1)\rangle = \frac{1}{\sqrt{2}}(|\Uparrow\Downarrow\rangle - |\Downarrow\Uparrow\rangle) \tag{2}$$
$$|T_+(1,1)\rangle = |\Uparrow\Uparrow\rangle \tag{3}$$
$$|T_0(1,1)\rangle = \frac{1}{\sqrt{2}}(|\Uparrow\Downarrow\rangle + |\Downarrow\Uparrow\rangle) \tag{4}$$
$$|T_-(1,1)\rangle = |\Downarrow\Downarrow\rangle \tag{5}$$
$$\tag{6}$$

Here, the arrows correspond to the spin of the electrons being up or down and the numbers i, j in $S(i, j)$ correspond to the number of electrons in each quantum dot.

The photons in the resonator are coupled to the DQD through their interaction and are either transmitted or reflected. Measuring these reflected photons, also known as the reflection coefficient, allows us to determine properties of the DQD, such as its spin, without collapsing the state of the DQD.

To simplify our calculations, we treat the system as a three level system containing the two singlet states and $T_-(11)$ state. When a magnetic field is applied the Hamiltonian of the system can be described by the following matrix:

$$H = \begin{pmatrix} 0 & \Delta & 0 \\ \Delta & -\epsilon & \Delta_{so} \\ 0 & \Delta_{so} & -\alpha \end{pmatrix} \tag{7}$$

We neglect the states $|T_{+}(1,1)\rangle$ and $|T_0(1,1)\rangle$ as they are not coupled to the singlet states.

The eigenenergies of such a system are graphed in Figure 2 for various values of magnetic field and spin orbit interaction, with zero external magnetic field applied.

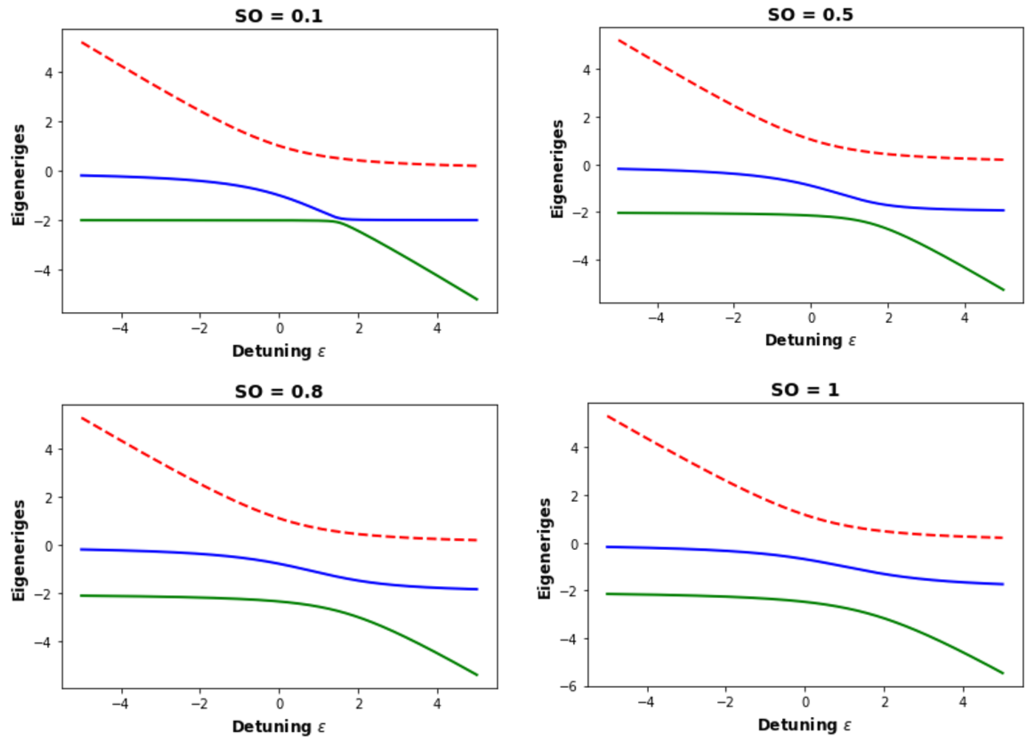

Figure 2: *Eigenenergies of Singlet and Triplet states for different Spin Orbit Interactions*

Here, ϵ is the energy of the single isolated quantum dot, $\alpha = \frac{1}{2}(g_1 + g_2)B$ is the energy of the triplet state and dependant on the magnitude of the magnetic field, B and the gyromatic ratios of the quantum dots, g_1 and g_2. In this Hamiltonian we have three states, two singlets and one triplet and a tunnel coupling between the two singlet states, which we call Δ. The term Δ_{so} corresponds to the spin orbit interaction between the singlet and one triplet state $T_{-}(1,1)$.

2 Input-Output Theory

To understand the multilevel system as described above, we first begin with the two level system of a quantum dot and superconducting resonator, and determine the relationship between the systems parameters and the reflection coefficient.

2.1 Heisenberg Langevin Equations of Motion

We start with the James Cummings Hamiltonian for a coupled system with of a quantum dot and resonator.

$$H_{tot} = \hbar\Delta_0 a^{\dagger} a + \frac{\hbar\Delta}{2}\sigma_z + \hbar g_{eff}(a\sigma_{+} + a^{\dagger}\sigma_{-}) \tag{8}$$

Here $\Delta_0 = \omega_0 - \omega_r$ is the cavity detuning from the field, a and σ are the ladder operators. We define $\Delta = \frac{\Omega}{\hbar} - \omega_r$, and $g_{eff} = g_c \frac{2t_C}{\Omega}$ where g_c is the coupling constant, t_C is the coherent tunneling matrix element and $\Omega = \frac{1}{2}\sqrt{\epsilon^2 + t_c^2}$ where ϵ is the detuning induced by the local gate voltages and the transmission line resonator.

This Hamiltonian can be rewritten as:

$$H = H_{sys} + H_I + H_C \tag{9}$$

where H_{sys} is the Hamiltonian of the isolated quantum dot, H_C is the Hamiltonian of the cavity, $H_I = \hbar g_{eff}(a\sigma_+ + a^\dagger \sigma_-)$ is the interaction Hamiltonian between the cavity and the resonator.

We first use Heisenberg equations of motion to obtain an equation of motion for each operator

$$\frac{dO_H}{dt} = -\frac{i}{\hbar}[O_H, H] + \frac{dO_S}{dt} \tag{10}$$

where O_H is the operator in the Heisenberg picture, which is obtained when applying a unitary matrix $UO_SU^\dagger$ to O_S, where O_S is the operator in the Schrodinger equations.

Here we assume that their is an exponential loss in the cavity with a cavity decay constant $\kappa = \kappa_1 + \kappa_{int}$, where κ_1 is the cavity constant due to the decay between the coupled fields and κ_{int} is due to any internal losses of the cavity. Using these assumptions in equation 10 we can therefore state:

$$\frac{da}{dt} = \frac{-i}{\hbar}[a, H] - \frac{\kappa}{2}a + \Gamma \tag{11}$$

Here, Γ is due to any noise fluctuations in the system.

As this is coupled to an external field, the only fluctuations that the cavity will experience is from the incoming wave. Because of this, we can then state $\Gamma = \gamma a_{in}$, where a_{in} is the incoming wave and γ is as yet undetermined.

We can therefore rewrite this equation 11 as

$$\frac{da}{dt} = -\frac{i}{\hbar}[a, H] - \frac{\kappa}{2}a + \gamma a_{in} \tag{12}$$

As this equation must be time symmetric we can reverse:

$$\frac{da}{d(-t)} = -\frac{i}{\hbar}[a, H] - \frac{\kappa}{2}a + \gamma' a_{out} \tag{13}$$

Using Equations 12 and 13 as well as the boundary condition at the point of contact between the external probing field and the cavity $a = k(a_{in} + a_{out})$, (where k is unknown), we can see that $\kappa \cdot k = \gamma'$ and $\gamma' = \gamma$. Inserting these into the equations we obtain: We can therefore rewrite this equation 11 as

$$\frac{da}{dt} = \frac{-i}{\hbar}[a, H] - \frac{\kappa}{2}a + \kappa \cdot k a_{in} \tag{14}$$

As this equation must be time symmetric we can reverse:

$$\frac{da}{d(-t)} = \frac{-i}{\hbar}[a, H] - \frac{\kappa}{2}a + \kappa \cdot k a_{out} \tag{15}$$

where k is undetermined.

Transformation to the Frequency Domain

We can transform to the frequency domain using the following relation:

$$a(\omega) = \frac{1}{\sqrt{2\pi}} \int_{-\infty}^{\infty} e^{i\omega t} a(t) dt \tag{16}$$

Inserting 16 into equation 14 we obtain

$$-i\Delta a(\omega) = \frac{-i}{\hbar}[a(\omega), H] - \frac{\kappa}{2}a(\omega) + \kappa \cdot k a_{in}(\omega) \tag{17}$$

Applying the creation and annihilation operators commutation relations with the Hamiltonian and exploiting the commutation relation

$$[a(\omega), a^\dagger(\omega')] = i\hbar\Delta\delta(\omega - \omega')$$

we obtain the following equations using the Hamiltonian as described in equation 8

$$-i\Delta_0 a(\omega) = -i\Delta_0 a(\omega) + \frac{\hbar\Delta}{2}\sigma_z - \frac{\kappa}{2}a(\omega) + \kappa \cdot k a_{in}(\omega) \tag{18}$$

Determining k

Taking k as the normalization constant for the internal normal mode we can then calculate its value using the relation $[a^\dagger(t), a(t)] = 1$.

Using this relation in the frequency domain as well as the commutation relations for $a(\omega)$, one obtains $k = \kappa^{-\frac{1}{2}}$. Inserting this into our equations of motion we obtain

$$\frac{da}{dt} = -i\Delta_0 a + ig_{eff}\sigma_- - \frac{\kappa}{2}a + \sqrt{\kappa}a_{in} \tag{19}$$

If there is more boundary's/external coupling fields, such as $a_{in,1}$ and $a_{in,2}$, this simply requires adding an additional term to equation 19 obtaining

$$\frac{da}{dt} = -i\Delta_0 a + ig_{eff}\sigma_- - \frac{\kappa}{2}a + \sqrt{\kappa_1}a_{in,1} + \sqrt{\kappa_2}a_{in,2} \tag{20}$$

One can also apply this method to the operator σ to obtain

$$\frac{d\sigma_z}{dt} = -i\Delta_0 a + ig_{eff}\sigma_- - \frac{\kappa}{2}\sigma_z \tag{21}$$

Here, we do not take into account any noise fluctuations in the two level system, thus eliminating Γ.

2.2 Derivation of the Transmission Coefficient S_{11}

Given the two Heisenberg Langevin Equations for this system:

$$\frac{da}{dt} = -i\Delta_0 a + ig_{eff}\sigma_- - \frac{\kappa}{2}a + \sqrt{\kappa_1}a_{in,1} + \sqrt{\kappa_2}a_{in,2} \tag{22}$$

$$\frac{d\sigma_z}{dt} = -i\Delta_0 a + ig_{eff}\sigma_- - \frac{\kappa}{2}\sigma_z \tag{23}$$

we can now determine $S_{11} = |\frac{a_{out,1}}{a_{in,1}}|^2$ by first eliminating time dependence from each equation. Rearranging equation 23, and setting $\sigma_z = -1$ (this assumes the electron is in the ground state), we then obtain

$$\sigma_- = a\frac{\Delta + \frac{i\gamma}{2}}{g_{eff}} = a\chi^{-1} \tag{24}$$

where $\chi = \frac{g_{eff}}{\Delta + \frac{i\gamma}{2}}$. Inserting this into equation 22 and assuming $a_{in,2} = 0$, we obtain

$$\frac{a_{out,2}}{a_{in,1}} = \frac{\sqrt{\kappa_1}}{i\Delta_0 + \frac{\kappa}{2} + ig_{eff}\chi} \tag{25}$$

Using the relation derived above, $a = \sqrt{\kappa_2}(a_{in,1} + a_{out,2})$, we can then find the matrix element S_{11} to be

$$S_{11} = |1 + \frac{i\kappa_1}{\Delta_0 - \frac{i\kappa}{2} + g_{eff}\chi}|^2 \tag{26}$$

In order to obtain a more general formalism of this for multilevel systems, we apply a new formalism, as described in the next section and in [2].

3 Multilevel Systems

In [2], a new formalism is developed which allows us to determine a relationship between the systems parameters and the transmission coefficient in the coupled resonator.

In doing so, the reflection coefficient of the system is found to be

$$S_{11} = |1 + \frac{i\kappa_1}{\Delta_0 - \frac{i\kappa}{2} + g^2\chi}|^2 \tag{27}$$

where χ is found to be

$$\chi(\omega) = \Sigma_{n,m} \frac{(p_n - p_m)|Z_{nm}|^2}{\omega + \Delta E_{nm} + \frac{i\gamma}{2}} \tag{28}$$

In deriving these equations, the following assumptions are made:

1. The assumption that the density matrix is diagonal in the basis of eigenvectors of the Hamiltonian, where $\rho = \Sigma_n p_n |n\rangle \langle n|$
2. The assumption that $H_{sys} |n\rangle = E_n |n\rangle$, where $|n\rangle$ are the eigenvectors and E_n are the eigenvalues of the systems Hamiltonian

We must therefore transform to eigenbasis of the Hamiltonian. In this new basis we assume that the Z_D matrix is diagonal and equivalent to σ_z in the given Fock space.

We require this matrix in our original basis in order to use equation 27. To do so we must transform back to our original basis using the transformation $Z = UZ_DU^\dagger$, where the unitary matrix U is composed of the eigenvectors of our Hamiltonian.

Using this Z matrix, we can then determine χ, the susceptibility for a given system.

3.1 Case Study I: Two Level System

We first investigate the two level system, and determine whether our new formalism agrees with the rotating wave approximation.

The Hamiltonian investigated is as follows:

$$H_{sys} = \begin{pmatrix} 0 & \Delta \\ \Delta & -\epsilon \end{pmatrix} \tag{29}$$

and the Z matrix in the Hamiltonian is given by:

$$Z_D = \begin{pmatrix} 1 & 0 \\ 0 & -1 \end{pmatrix} \tag{30}$$

Finding the eigenvectors of H_{sys} and transforming the Z matrix back to our original basis, we obtain the elements Z_{nm} to determine $\chi(\omega)$. This can be derived analytically and was found to be:

$$\chi(\omega) = \frac{\Delta p_{01}|Z_{01}|^2}{\omega + \Delta E_{nm} + \frac{i\gamma}{2}} - \frac{\Delta p_{01}|Z_{10}|^2}{\omega + \Delta E_{nm} + \frac{i\gamma}{2}} \tag{31}$$

$$\chi(\omega) = \Delta p_{01}\left(\frac{1}{\omega + \Omega + \frac{i\gamma}{2}} - \frac{1}{\omega - \Omega + \frac{i\gamma}{2}}\right) = \chi_{01} - \chi_{10} \tag{32}$$

where $\Omega = \sqrt{\epsilon^2 + 4\Delta^2}$. Note that we have used $\Delta p_{ij} = -\Delta p_{ji}$.

This implies we have the S_{11} element for the following Hamiltonian to be:

$$S_{11} = |1 + \frac{i\kappa_1}{\Delta_0 - \frac{i\kappa}{2} + g^2(\chi_{01} - \chi_{10})}|^2 \tag{33}$$

To confirm our approach, we also plot g_{eff} and χ for this two level system, as shown in Figure 3

3.2 Case Study II: Three Level System

We now apply this new formalism for the three level system, which contains two singlets and one triplet. The Hamiltonian is given again below and described in equation 34.

$$H = \begin{pmatrix} 0 & \Delta & 0 \\ \Delta & -\epsilon & \Delta_{so} \\ 0 & \Delta_{so} & -\alpha \end{pmatrix} \tag{34}$$

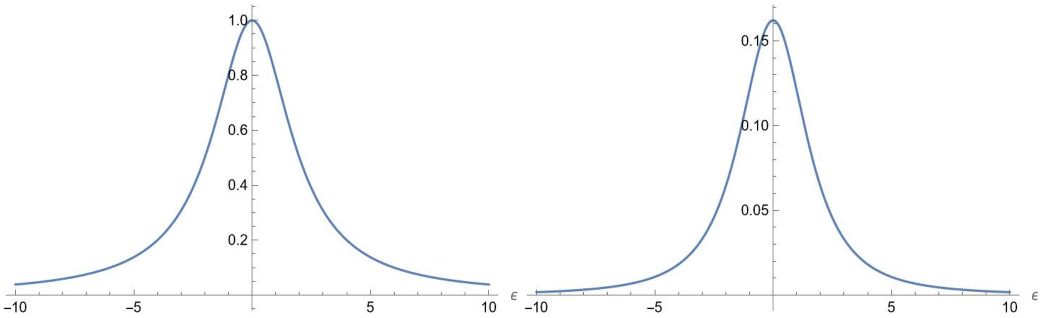

(a) *g_{eff} plotted as a function of detuning with $\Delta = 1$, $\alpha = 0.1$*
(b) *χ plotted as a function of detuning with $\Delta = 1$, $\alpha = 0.1$*

Figure 3: *Both g_{eff} and χ plotted as a function of detuning*

The Z matrix in the basis of the eigenvectors is given by

$$Z_D = \begin{pmatrix} 1 & 0 & 0 \\ 0 & -1 & 0 \\ 0 & 0 & 1 \end{pmatrix} \tag{35}$$

Here, we use the same parameters as described in the table below. These were the given parameters of all graphs unless otherwise stated.

Parameters List		
Parameter Name	**Symbol**	**Value**
Tunnel Coupling	Δ	1
Gyromatic ratios	g_1, g_2	2, 2.01
Coupling Coefficient	g_c	0.1
Temperature	T	0.1
Cavity Decay Constants	κ_1, κ_2	0.001, 0.001
Coherence	γ	0.1
Spin Orbit Coupling Coefficient	Δ_{so}	0.1
Frequencies of Qubit and Cavity	ω, ω_0	0.0101, 0.0100

We numerically find the eigenvectors of this system and transform Z_D in the original basis, to determine the Z_{mn} elements in χ. The equation of χ for the three level system is then given by

$$\begin{aligned} \chi(\omega) \quad = \quad & \Delta p_{01}\left(\frac{|Z_{01}|^2}{\omega + \Delta E_{01} + \frac{i\gamma}{2}} - \frac{|Z_{10}|^2}{\omega + \Delta E_{10} + \frac{i\gamma}{2}}\right) \\ & + \Delta p_{12}\left(\frac{|Z_{12}|^2}{\omega + \Delta E_{12} + \frac{i\gamma}{2}} - \frac{|Z_{21}|^2}{\omega + \Delta E_{21} + \frac{i\gamma}{2}}\right) \end{aligned}$$

Note that the above equation is only for this particular system and different Hamiltonian's will correspond to different susceptibilities.

Inserting this into equation 33, we can determine the relationship between different parameters of the system and the transmission coefficient of the matrix.

The transmission coefficient was numerically calculated for a variety of different magnetic fields and detuning. An example of results can be seen below in Figure 4, where all parameters used are as described in the table above.

4 Parameter Sweeps

First, parameter sweeps were carried out for the two level system, for a range of values of detuning between the two dots ϵ and magnetic field B. Unless otherwise stated the parameters in the equations above were as seen in Table below. All sweeps were calculated numerically using Python.

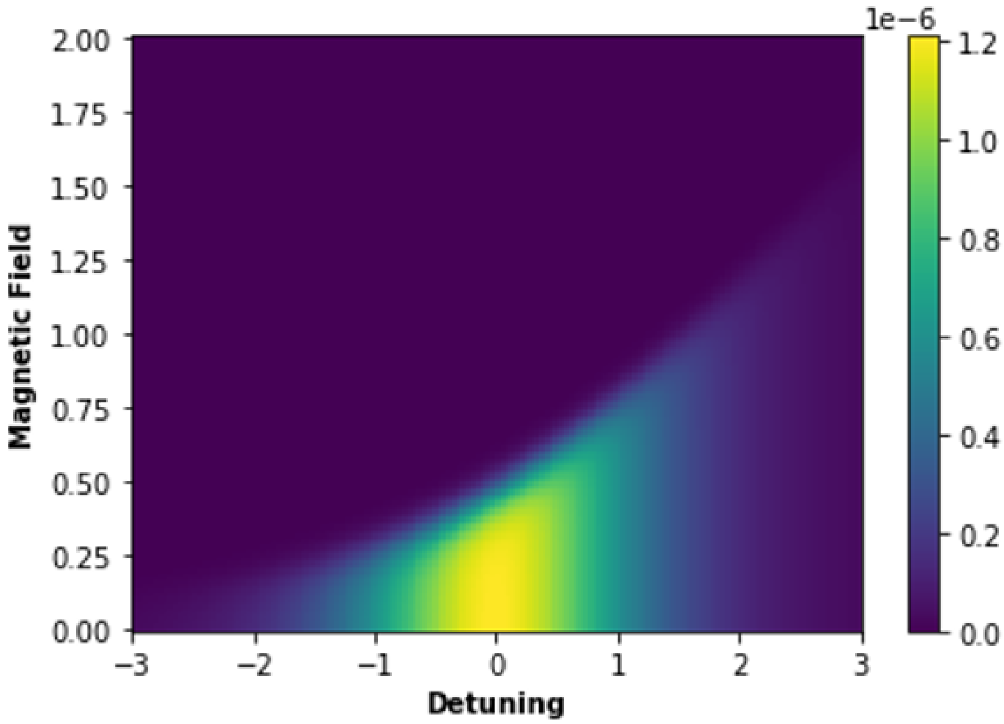

Figure 4: *Transmission Coefficient as a function of Magnetic Field and Detuning*

4.1 Temperature Sweep for Case Study I

The results of increasing temperature on the two level system can be seen in Figure 5

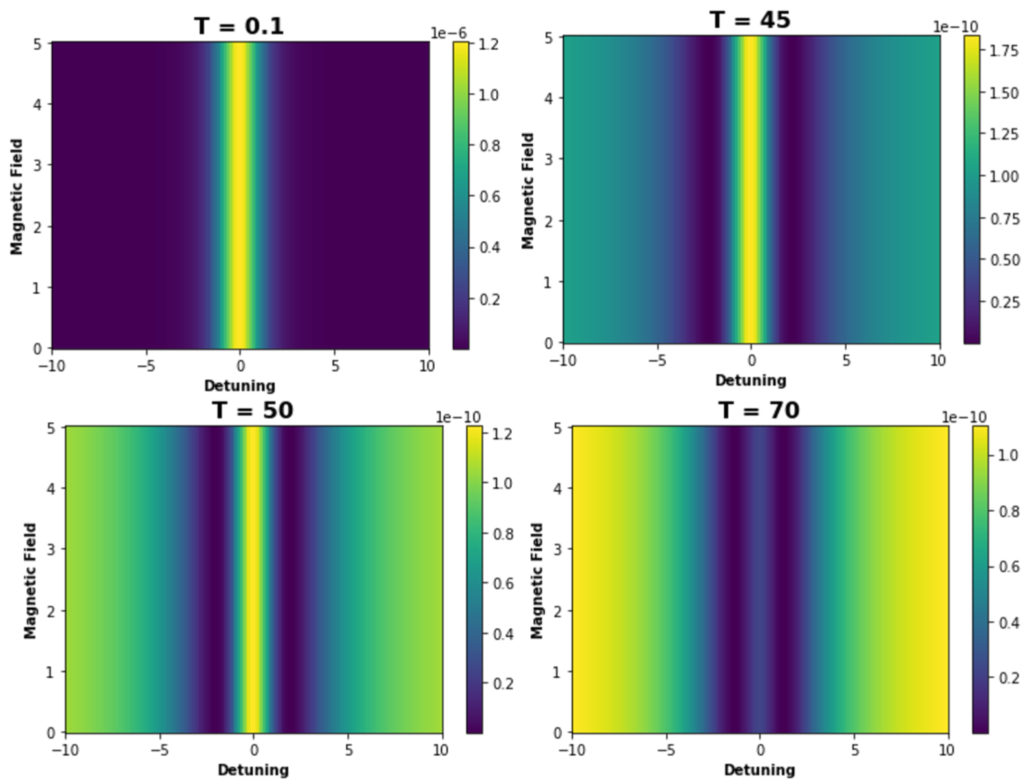

Figure 5: *Transmission Coefficient as a function of Magnetic Field and Detuning for Case Study I*

One can see from Figure 5 as we increase the temperature, the area at which the transmission matrix is at a maximum splits in two.

4.2 Temperature Sweep for Case Study II

The temperature dependence of the system is seen through the probabilities of the different levels. Here we assume a thermal distributions, where

$$p_i = \frac{e^{\frac{-E_i}{k_b T}}}{Z}$$

Here, E_i are the eigenenergies corresponding to each system, T is the temperature, Z is the partition function of the system and k_b is the Boltzmann Constant.

A sweep of a range of temperatures were taken and can be seen below in Figure 6

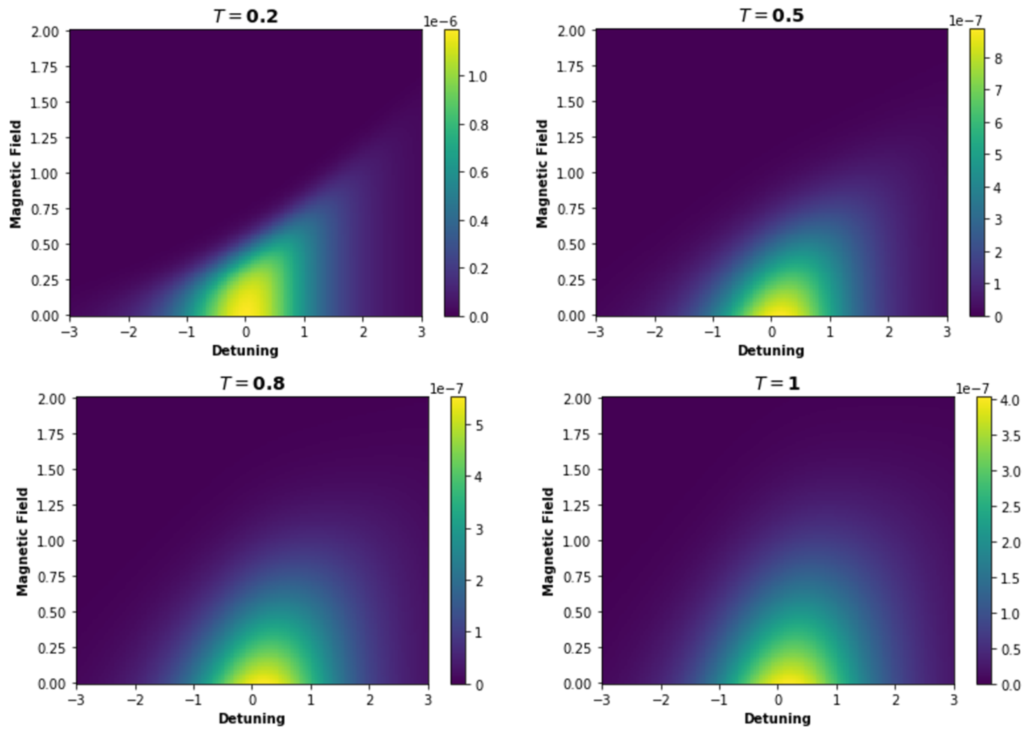

Figure 6: *Reflection Coefficient as a function of Magnetic Field and Detuning for various temperatures*

It is evident from Figure 6 that as one increases the temperature, she sharp change in the reflection coefficient disappears.

This is due to the populations of each level increasing. At low temperatures $S_{-}(0,2)$ is populated while the other two levels are empty. Therefore as we increase the magnetic field and the $T_{-}(1,1)$ energy level shifts downwards, and leads to the sharp transition in the reflection coefficient. If we increase the temperature the population of the lower energy level decreases, while the other two increase, as seen in Figure 7.

This would imply that as the magnetic field decreases and the triplet state travels downwards in the energy spectrum, there is still some populous energy levels, which leads to the 'blurring' effect observed in figures 6.

The magnetic field $B = 1$ was set and a sweep of the reflection coefficient and detuning was then taken, which can be seen below in Figure 8

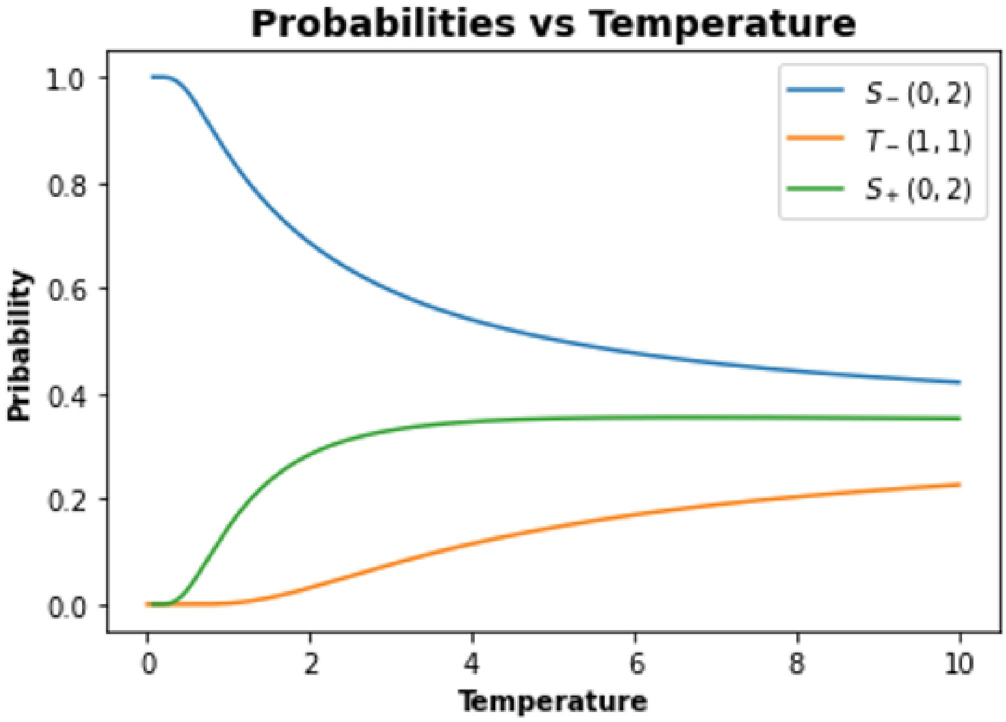

Figure 7: *Population Levels as a function of temperature for the three different levels*

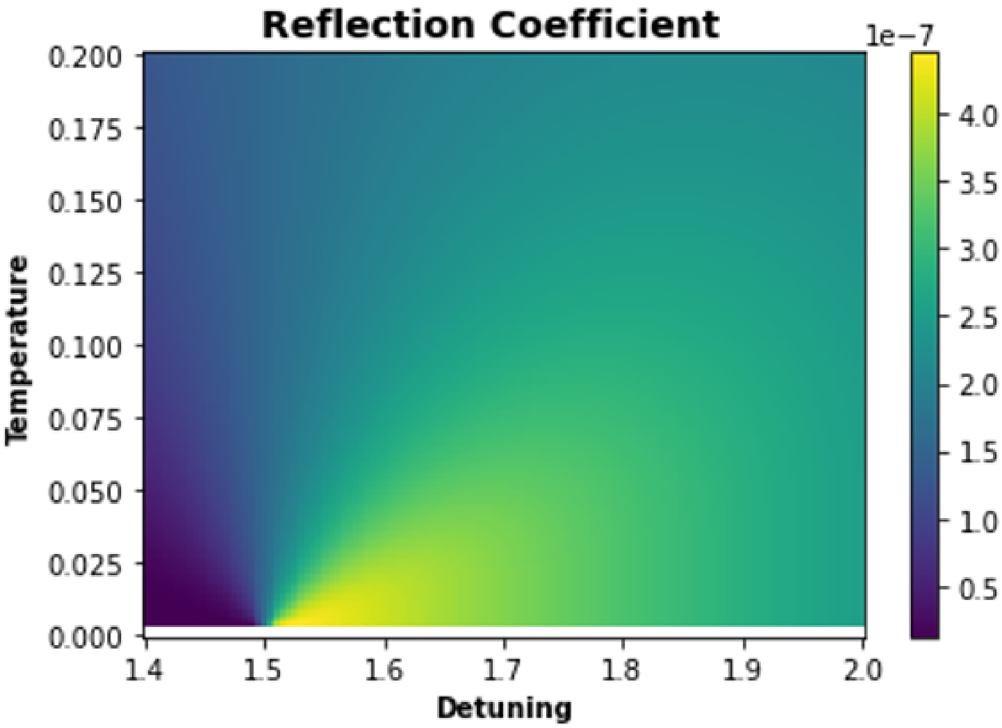

Figure 8: *The reflection coefficient as a function of detuning and temperature*

.

4.3 Coherence Sweep for Case Study I

We then investigate the difference between the coherent and decoherent regime for the system, and complete a sweep of the parameter γ, again over a range of detuning and magnetic field. The full sweep can be seen in Figure 12.

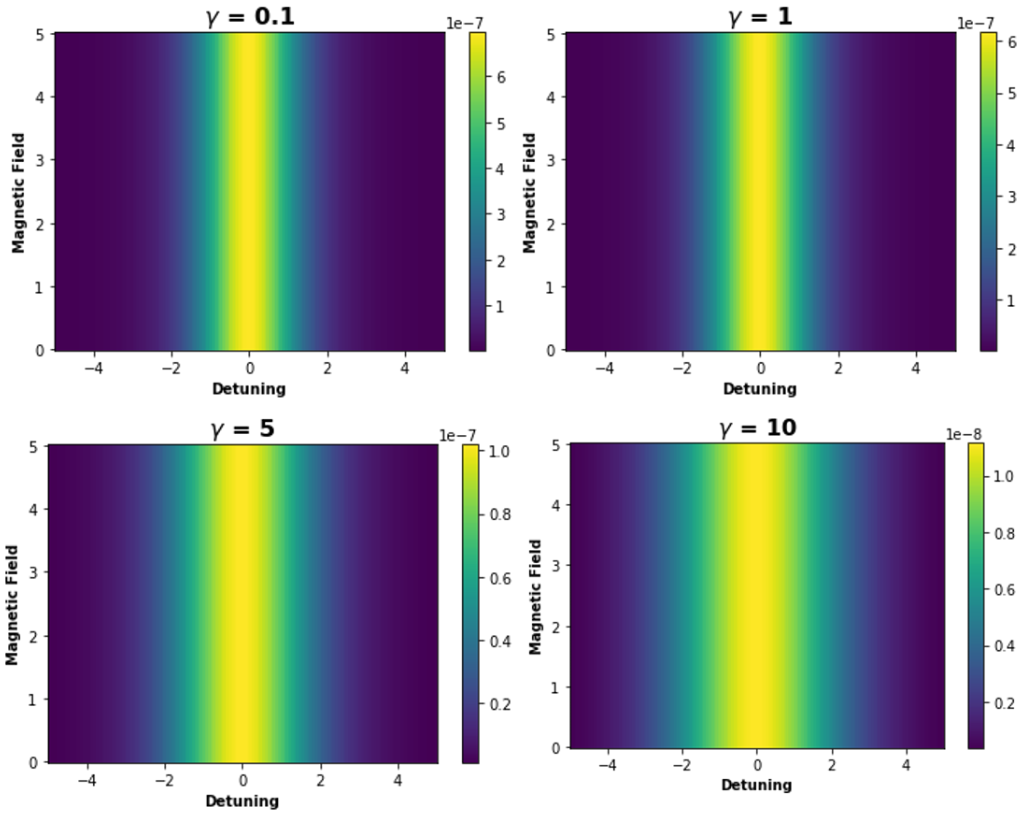

Figure 9: *Transmission Coefficient as a function of Magnetic Field and Detuning for various coherence's for a Two Level System*

One can see that as we increase the parameter γ, or decrease the coherence of the system, one can see that the range of detuning at which we get a large reflection coefficient increases.

4.4 Coherence Sweep for Case Study II

A sweep of coherence was carried out for Case Study II, which can be seen in Figure 10.

Here, we can also see that as we decrease the coherence of the system by increasing γ, we can see that the range of detuning values with high reflection coefficient also increases.

This shows that as we increase γ, the DQD loses phase and becomes decoherent. This corresponds to a larger range of detuning parameters at which the reflection coefficient is measured.

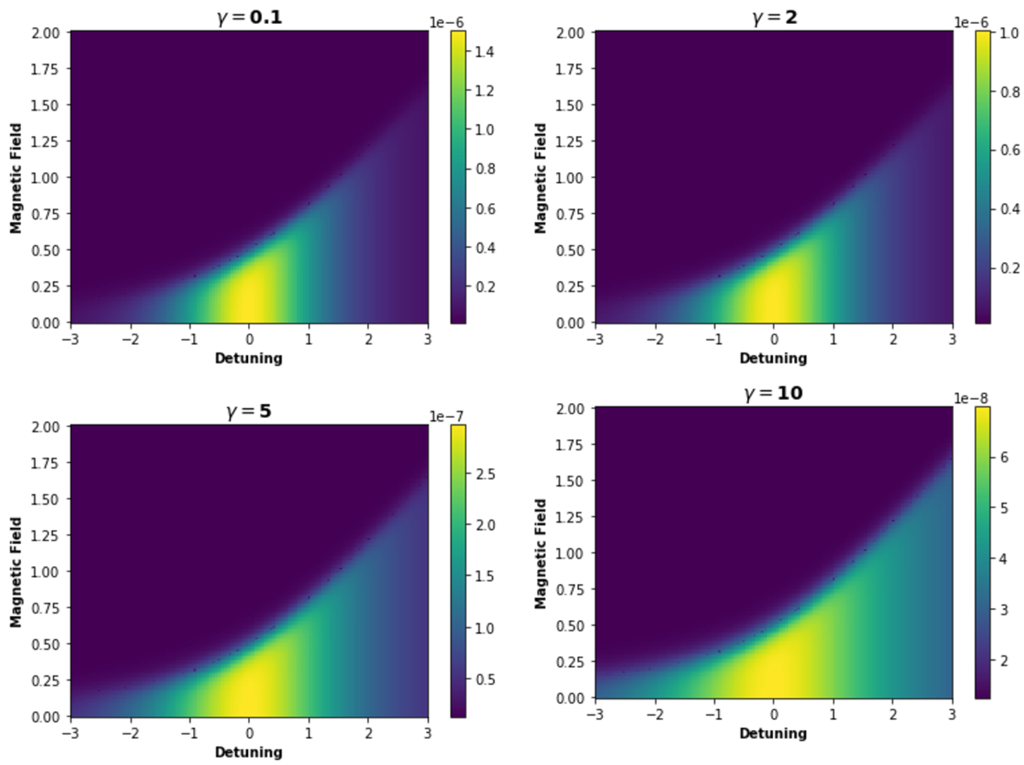

Figure 10: *Sweep of different coherence for Case Study II*

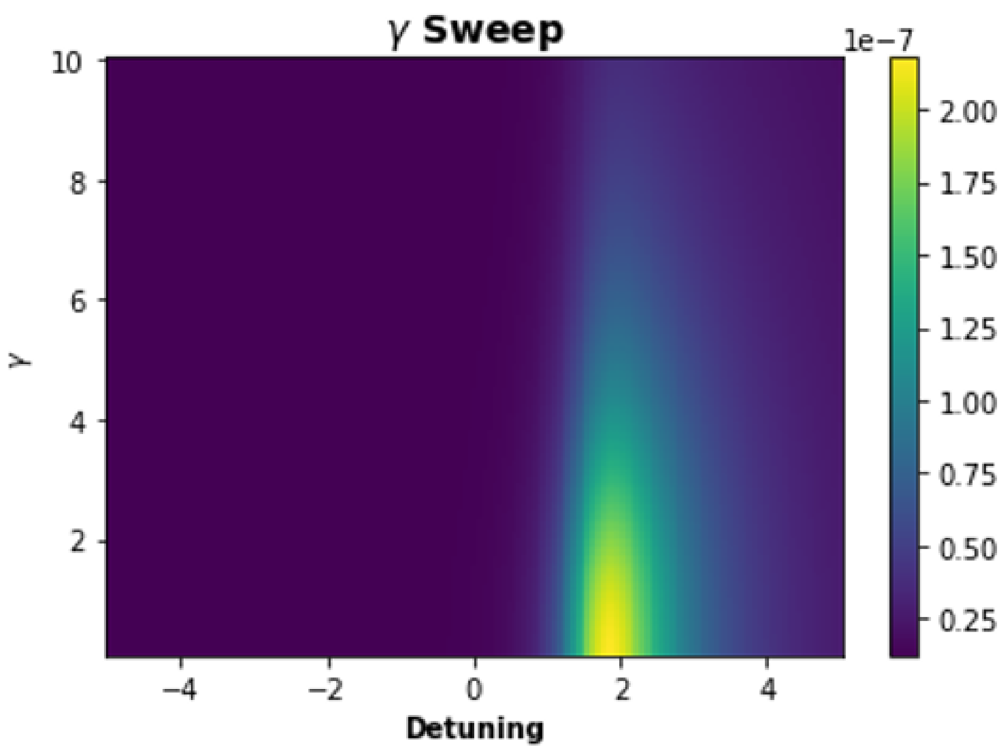

Figure 11: *Reflection Coefficient as a function of detuning and Coherence*

4.5 Frequency Sweep for Case Study I

A sweep of the frequency of the resonator is also carried out for a range of different magnetic fields and detuning parameters for the two level system, which can be seen in Figure 12. One can see as we increase the frequency of the resonator, the range of detuning at which we get a reflected signal increases until it eventually splits in two.

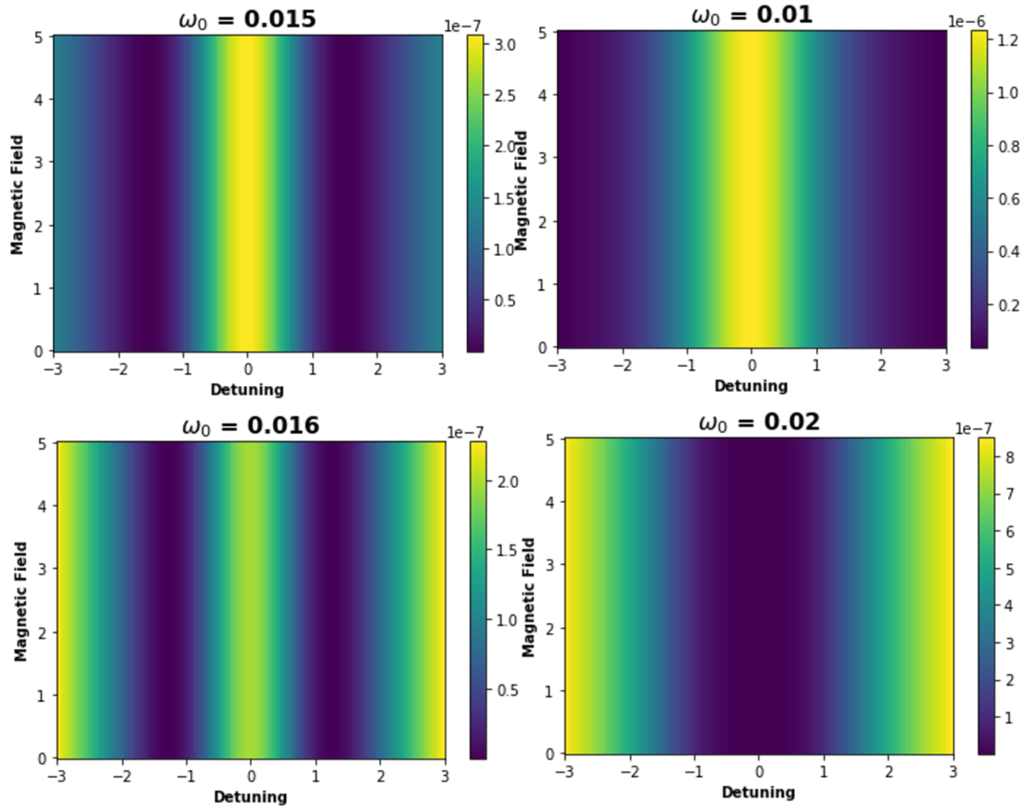

Figure 12: *Transmission Coefficient as a function of Magnetic Field and Detuning for various different cavity frequencies for the Two Level System*

4.6 Frequency Sweep for Case Study II

The reflection coefficient as a function of magnetic field and detuning is seen below in Figure 13

The reflection coefficient can also be seen as a function of cavity frequency and detuning can be seen below with the magnetic field $B = 1$, as seen in Figure 14.

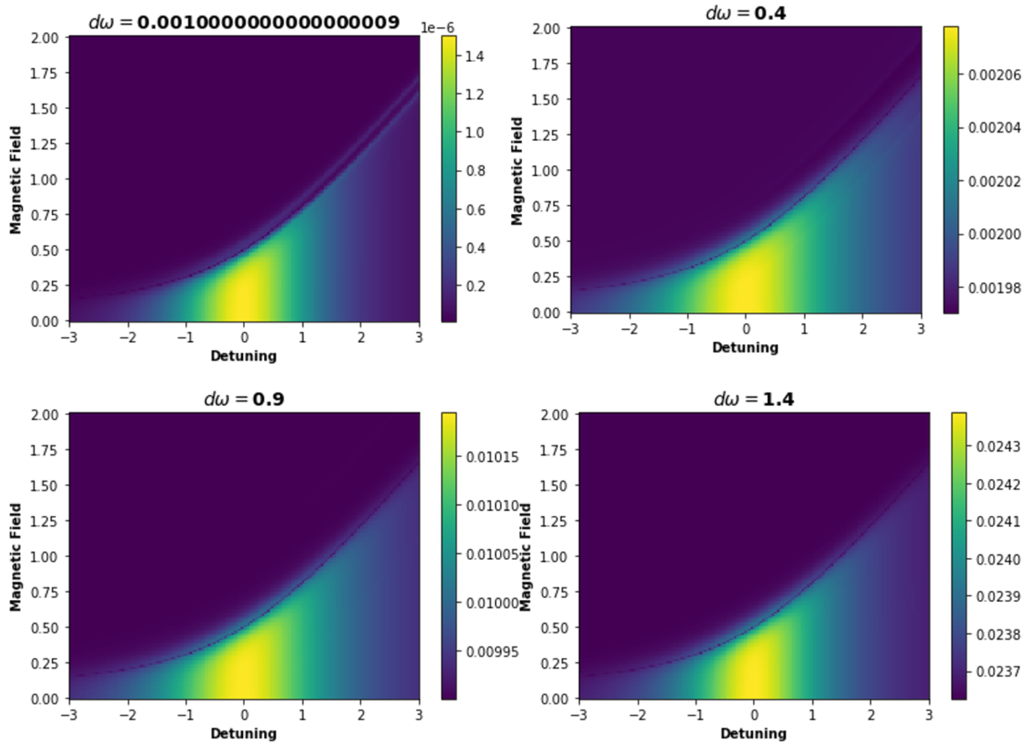

Figure 13: *Reflection Coefficient as a function of detuning and cavity frequencies for B = 1*

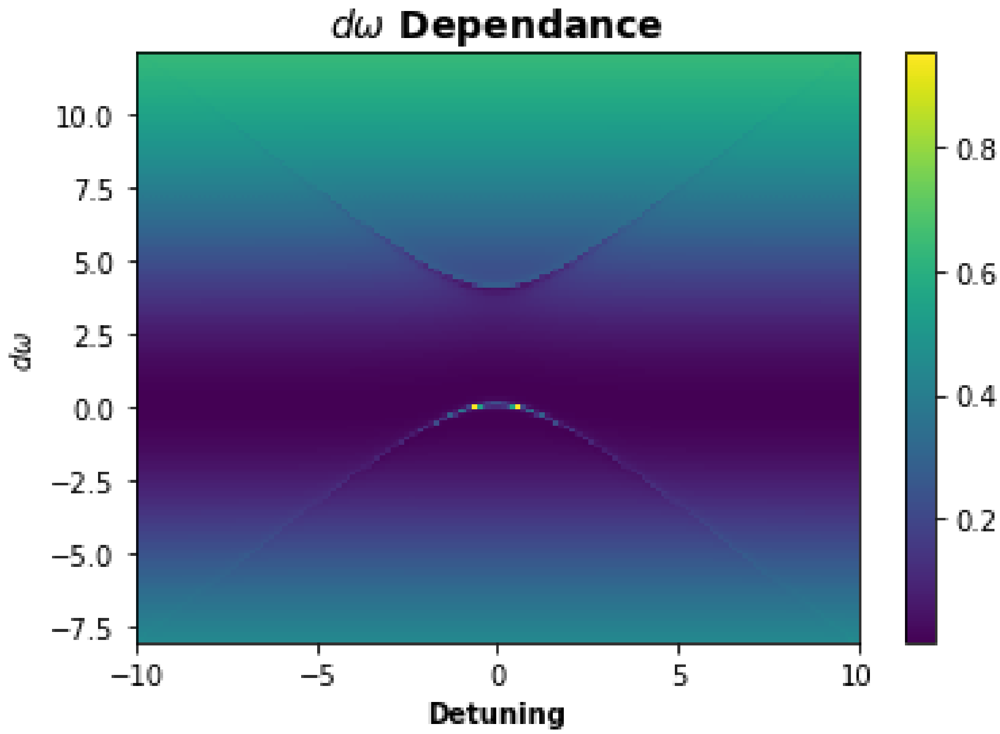

Figure 14: *Reflection Coefficient as a function of detuning and magnetic field for a variety of different cavity frequencies.*

.

4.7 Sweep of Spin Orbit Interaction in Case Study II

In figure 15, the reflection coefficient as a function of detuning and magnetic field for various different spin orbit couplings is seen below

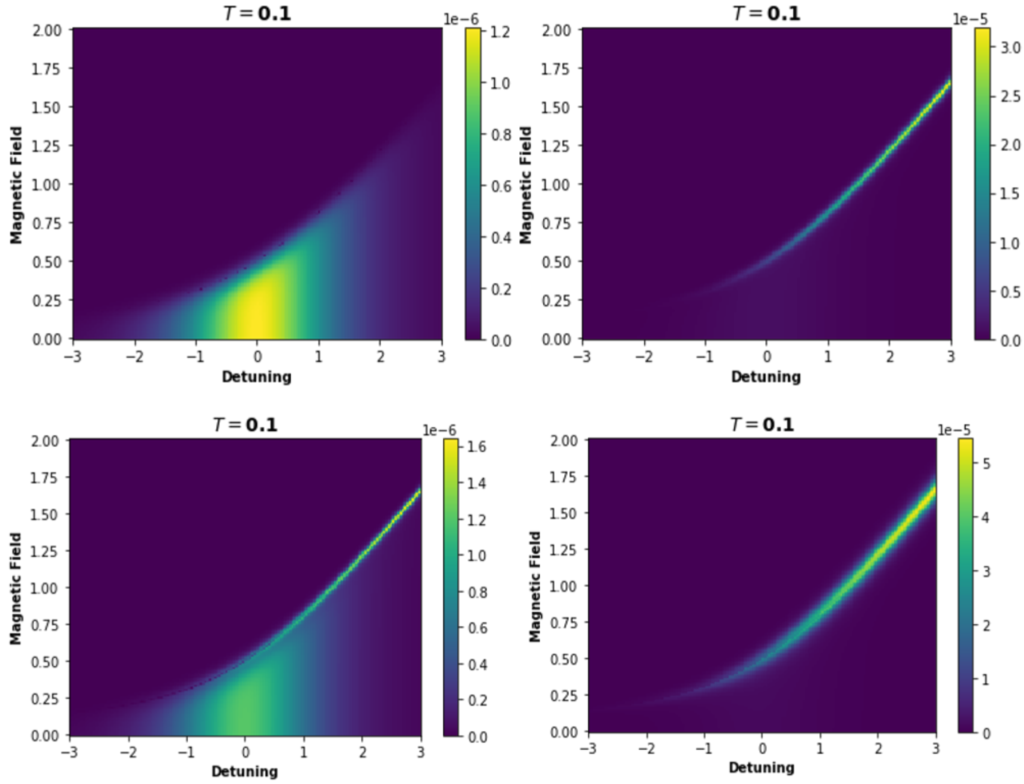

Figure 15: *Reflection Coefficient as a function of detuning and magnetic field with various different spin orbit couplings*

It is evident that as we increase the value of the spin orbit coupling, the triplet state begins to dominate and the singlet state begins to fade. Observing these in the energy diagram in figure 16 one finds that, as the spin orbit coupling parameter increases, the triplet and singlet state become further apart, leading to a more cut straight edge on the energy level of the lowest level, i.e. $S_{-}(0, 2)$.

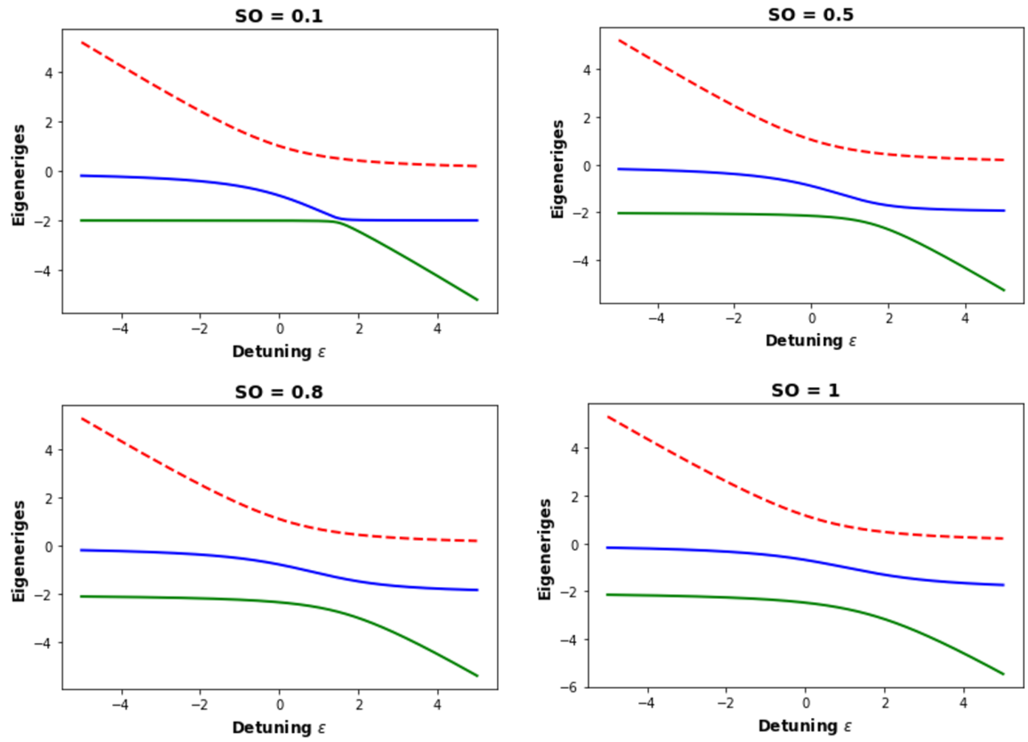

Figure 16: *Energy Levels of three systems with different spin orbit couplings*

Bibliography

[1] M. Benito et al. "Input-output theory for spin-photon coupling in Si double quantum dots". In: *Phys. Rev. B* 96 (23 Dec. 2017), p. 235434. DOI: 10.1103/PhysRevB.96.235434. URL: https://link.aps.org/doi/10.1103/PhysRevB.96.235434.

[2] Sigmund Kohler. "Dispersive readout: Universal theory beyond the rotating-wave approximation". In: *Physical Review A* 98.2 (Aug. 2018). ISSN: 2469-9934. DOI: 10.1103/physreva.98.023849. URL: http://dx.doi.org/10.1103/PhysRevA.98.023849.

[3] David J. Ibberson et al. "Large Dispersive Interaction between a CMOS Double Quantum Dot and Microwave Photons". In: *PRX Quantum* 2 (2 May 2021), p. 020315. DOI: 10.1103/PRXQuantum.2.020315. URL: https://link.aps.org/doi/10.1103/PRXQuantum.2.020315.